arXiv:1311.1385v1 [astro-ph.SR] 6 Nov 2013

HIGH-PRECISION 2MASS JHK_S LIGHT CURVES AND OTHER DATA FOR RR LYRAE STAR SDSS$J015450 + 001501$: STRONG CONSTRAINTS FOR NON-LINEAR PULSATION MODELS

Róbert Szabó[1], Željko Ivezić[1,2], László L. Kiss[1,3,4], Zoltán Kolláth[1,5], Lynne Jones[2], Branimir Sesar[6], Andrew C. Becker[2], James R.A. Davenport[2], and Roc M. Cutri[7]

Draft version November 7, 2013

ABSTRACT

We present and discuss an extensive data set for the non-Blazhko ab-type RR Lyrae star SDSS$J015450 + 001501$,including optical SDSS $ugriz$ light curves and spectroscopic data, LINEAR and CSS unfiltered optical light curves, and infrared 2MASS JHK_s and WISE W1 and W2 light curves. Most notably, light curves obtained by 2MASS include close to 9000 photometric measures collected over 3.3 years and provide exceedingly precise view of near-IR variability. These data demonstrate that static atmosphere models are insufficient to explain multi-band photometric light curve behavior and present strong constraints for non-linear pulsation models for RR Lyrae stars. It is a challenge to modelers to produce theoretical light curves that can explain data presented here, which we make publicly available.

Subject headings: stars: variables: RR Lyrae — infrared: stars — techniques: photometric — stars: atmospheres — stars: individual(SDSS$J015450 + 001501$) — stars: oscillations

1. INTRODUCTION

RR Lyrae stars are old low-mass (around half the Sun's) pulsating horizontal branch stars of spectral class A and F. They are important both as stellar evolutionary probes and as tracers of Galactic structure. For these reasons, accurate pulsational models for RR Lyrae stars are crucial in a large number of astrophysical applications. Marconi (2009) recently pointed out that a non-local time-dependent treatment of convection in non-linear (i.e., without small oscillation approximation) pulsation models for RR Lyrae are needed to explain the morphological characteristics of the variation along a pulsation cycle of luminosity, radius, radial velocity, effective temperature and surface gravity: "the comparison between theoretical and observed variations represents a powerful tool to constrain the intrinsic stellar parameters including the mass."

Precise multi-band light curves provide strong constraints for pulsation models. Bono et al. (2000) performed simultaneous fitting of multi-band ($UBVK$) light curves of an RRc star (U Comae). They transformed the bolometric magnitudes supplied by a hydrocode to standard magnitudes using bolometric corrections and empirical color-temperature relations based on `ATLAS9` model atmospheres (Castelli et al. 1997). Dorfi & Feuchtinger (1999) carried out detailed frequency-dependent radiative transfer computations to obtain UBVI light curves

of both RRab and RRc stars. Motivated by their results, in this work we present light curves for an RR Lyrae star pulsating in the fundamental mode (RRab) obtained over 15 years in ten photometric bandpasses that span more than a factor of ten in wavelength, and bracket the wavelength range where most of its luminosity is emitted. Most notably, light curves obtained by 2MASS include close to 9000 photometric measures obtained over 3.3 years and, after data averaging, provide exceedingly precise view of near-IR variability. While quasi-continuous, extreme precision optical ligth curves have recently become available thanks to the *Kepler* mission (*e.g.* ~ 140000 short cadence data points were analyzed for RRab stars FN Lyr and AW Dra in Nemec et al. (2011) and half a million points per star were discussed in Nemec et al. (2013)), we believe that a data set of similar completeness, precision, and wavelength and temporal coverage does not exist for any other RR Lyrae star in the near-infrared bandpasses. Hence, data presented here will provide unprecedented observational constraints for non-linear pulsation models of RR Lyrae stars and will stimulate modelers to include a self-consistent and frequency-dependent treatment of radiation hydrodynamics in the outer parts of these pulsators.

In §2 we present and analyze the available data, which we make public, and discuss and summarize our findings in §3.

2. DATA ANALYSIS

We first describe optical SDSS $ugriz$ light curves and spectroscopic data, LINEAR and CSS unfiltered light curve data, infrared 2MASS JHK_s and WISE W1 and W2 light curve data, and then perform their joint analysis. The temporal coverage and sizes of these data sets are summarized in Table 1.

As photometric data for RR Lyrae stars have been historically taken predominantly in the UBVRI system, it might be interesting to note that Ivezić et al. (2007) provide a set of non-linear transformation between BVRI and SDSS $griz$ magnitudes. For a linear transformation

[1] Konkoly Observatory, MTA CSFK, Konkoly Thege Miklós út 15-17, H-1121, Budapest, Hungary; rszabo@konkoly.hu
[2] Astronomy Department, University of Washington, Box 351580, Seattle, WA 98195-1580
[3] Sydney Institute for Astronomy, School of Physics, University of Sydney, NSW 2006, Australia
[4] ELTE Gothard-Lendület Research Group, Szent Imre herceg út 112, H-9700 Szombathely, Hungary
[5] University of West Hungary Savaria Campus, Szombathely, Hungary
[6] Division of Physics, Mathematics and Astronomy, Caltech, Pasadena, CA 91125
[7] Infrared Processing and Analysis Center, California Institute of Technology, Pasadena, CA 91125

Table 1
Photometric data analyzed in this work

Survey	MJD$_{min}^a$	MJD$_{max}^b$	N epochs^c	N data^d
2MASS	50660	51869	2969	8907
SDSS	51075	54412	64	320
LINEAR	52608	54817	225	225
CSS	53627	56297	270	270
WISE	55209	55575	43	86

^{a} Earliest MJD in the survey.
^{b} Latest MJD in the survey.
^{c} The number of photometric epochs.
^{d} The number of photometric data points (the number of epochs times the number of bandpasses).

between the U and u magnitudes the interested reader is referred to Jester et al. (2005).

2.1. SDSS data

The Sloan Digital Sky Survey (SDSS; Abazajian et al. 2009) has repeatedly imaged about 300 sq. deg. large equatorial strip limited by $309° <$ R.A. $< 60°$ and $|Dec| < 1.26°$, and known as Stripe 82. The properties of this data set and its impact on variability studies are discussed in detail by Ivezić et al. (2007), Sesar et al. (2007) and Bramich et al. (2008). An extensive study of light curves for RR Lyrae stars found in Stripe 82 was undertaken by Sesar et al. (2010).

The star discussed here was identified in SDSS Stripe 82 data with coordinates (J2000.0): R.A. = 28.709054 and Dec= +0.250206 (decimal degrees). Following standard SDSS nomenclature, hereafter we refer to it as SDSS$J015450 + 001501$. All SDSS data for this star are publicly[8] available, as well as published along with this paper electronically for convenience. Table 6 shows the form and content of the data. Images show a distinctively blue isolated point source, with the nearest brighter object more than 30 arcsec away. Its SDSS r band magnitude varies from ~14.6 to ~15.5 and, according to Sesar et al. (2010), this star is at a heliocentric distance of $D = 7.59$ kpc.

2.1.1. Imaging data

SDSS imaging data for this star were obtained 64 times and include nearly-simultaneous $ugriz$ photometry precise to 0.01-0.02 mag. In order to construct phased light curves, we use the period and epoch of maximum determined using better sampled LINEAR data (see §2.2). Phased and normalized SDSS urz light curves are shown in Fig. 1. Following Sesar et al. (2010), we normalized light curves by their amplitude (with minimum and maximum brightness determined using B splines) and shifted so that minimum brightness is 0 and maximum brightness is 1. As evident from Fig. 1, light curves are typical for ab RR Lyrae stars and greatly vary with wavelength.

2.1.2. Spectroscopic data

SDSS$J015450 + 001501$ was spectroscopically targeted by SDSS as a quasar candidate. Its SDSS spectrum (identifiers: plate=700, fiber=515, MJD=52199) is consistent with that for an A0 star (see Fig. 2). The spectroscopic parameters determined by the SEGUE Stellar
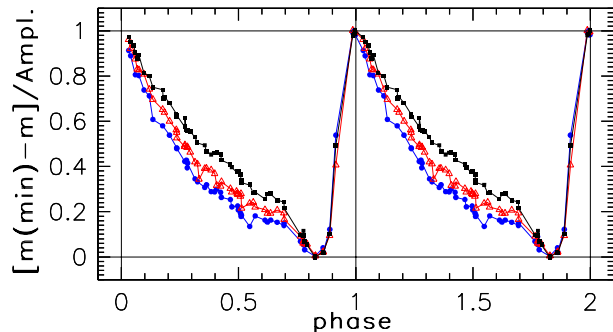
[8] http://skyserver.sdss3.org/dr9/en/tools/explore/obj.asp?sid=788271533805037568

Figure 1. Phased and normalized SDSS urz (bottom to top, respectively) light curves for SDSS$J015450 + 001501$. Data points are shown by symbols and connected by straight lines. The scatter is due to random photometric errors (0.01-0.02 mag).

Table 2
LINEAR light curve for RR Lyrae star
SDSS$J015450 + 001501$ (225 epochs)

MJD	mag	mag$_{err}$
52608.145642	15.559	0.257
52608.175414	15.424	0.024
...	...	...

Note. — For details see Sesar et al. (2011, 2013). Table 2 is published in its entirety in the electronic edition of the Journal. A portion is shown here for guidance regarding its form and content.

Parameter Pipeline (Lee et al. 2011) include $[Fe/H] = -1.31 \pm 0.03$, log(g)=2.97±0.20, T_{eff}=6580±104 K, and radial velocity -135.1 ± 1.8 km s^{-1}. We note however that the spectrum of this star is a coadd of 5 individual exposures, and the time between the start of the first and the end of the last exposure is 1.03 days. Thus, the parameters derived from this spectrum might contain much higher systematic errors because the individual exposures span a wide range of pulsational phases.
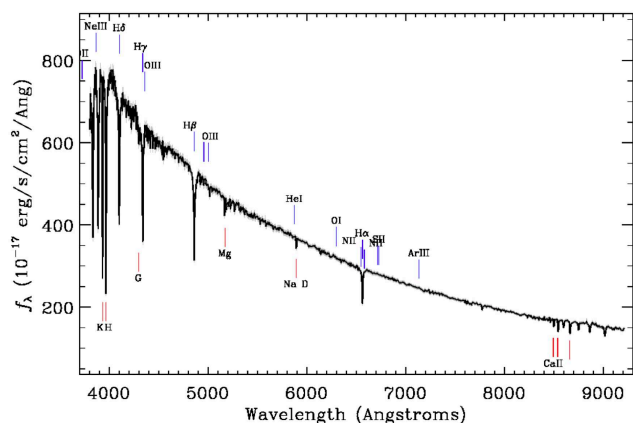

Figure 2. Default SDSS visualization of the SDSS spectrum for SDSS$J015450 + 001501$. The spectrum is classified as an A0 star.

2.2. LINEAR and CSS light curve data

The asteroid survey LINEAR was photometrically recalibrated by Sesar et al. (2011) using SDSS stars acting as a dense grid of standard stars. In the overlapping

Table 3
CSS light curve for RR Lyrae star
SDSS$J015450 + 001501$ (270 epochs)

MJD	mag	mag$_{\rm err}$
53710.18424	15.44	0.06
53710.19176	15.46	0.06
...	...	...

Note. — Table 3 is published in its entirety in the electronic edition of the Journal. A portion is shown here for guidance regarding its form and content.

$\sim$10,000 deg^2 of sky between LINEAR and SDSS, photometric errors for unfiltered (white light) photometry range from $\sim$0.03 mag for sources not limited by photon statistics to $\sim$0.20 mag at $r = 18$ (here r is the SDSS r band magnitude). LINEAR data provide time domain information for the brightest 4 magnitudes of SDSS survey, with 250 unfiltered photometric observations per object on average. The public access to the recalibrated LINEAR data is provided through the SkyDOT Web site (https://astroweb.lanl.gov/lineardb/) and is also available as auxiliary material with this paper (see Table 2). RR Lyrae stars from this data set have been analyzed by Sesar et al. (2013).

The Catalina Sky Survey (CSS) uses three telescopes to search for near-Earth objects. Each of the survey telescopes is run as separate sub-surveys, including the Catalina Schmidt Survey and the Mount Lemmon Survey in Tucson, Arizona, and the Siding Spring Survey in Siding Spring, Australia. CSS is similar to LINEAR in that it uses unfiltered observations and delivers similar photometric precision (but is deeper by several magnitudes). RR Lyrae stars from this data set have been analyzed by Drake et al. (2013).

SDSS$J015450 + 001501$ was observed by LINEAR and CSS about 500 times over 10 years. Both light curves are shown in Fig. 3 and are barely distinguishable. Using only LINEAR data, Sesar et al. (2013) have determined a best-fit period, $P = 0.636985$ day, and the epoch of maximum, MJD$_{\rm max} = 53675.299080$. Based on Sesar et al. (2011) photometric transformations between LINEAR and SDSS r-band data, a great degree of similarity is expected between unfiltered LINEAR/CSS light curves and the SDSS r-band light curve. This expectation is verified by data, as illustrated in Fig. 3. CSS observations of SDSS$J015450 + 001501$ are collected in Table 3.

2.3. 2MASS light curve data

The most extensive data set presented here comes from the 2MASS survey (Skrutskie et al. 2006). SDSS$J015450 + 001501$ falls in one of the 35 2MASS calibration fields that were imaged repeatedly in the J, H and K$_s$ bandpasses during each night of the 3.5 year survey. Full details are given in the online Explanatory Supplement[9] and Cutri et al. (2003). Analysis of various variable stars contained in this data set was presented by Plavchan et al. (2008), Becker et al. (2008) and Davenport et al. (2012), where more technical details can be found.

[9] http://www.ipac.caltech.edu/2mass/releases/allsky/doc/sec3_2d.html
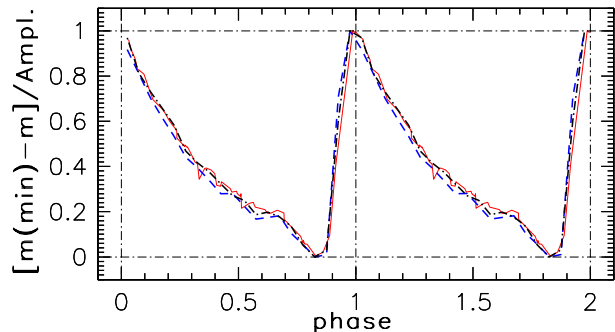

Figure 3. LINEAR (dashed), CSS (dot-dashed) and SDSS r-band (solid) light curves for SDSS$J015450 + 001501$. LINEAR and CSS data (225 and 270 data points, respectively) are median-ed in 0.05 wide phase bins, with resulting random errors at most 0.01 mag. SDSS light curve corresponds to 64 data points (with random errors of 0.01-0.02 mag) connected by straight lines (same curve as in Figure 1). Note that all three light curves barely differ from each other.

SDSS$J015450+001501$ was observed about 3,000 times in each of the three bandpasses (see Tables 1 & 7). Phased and normalized 2MASS light curves are shown and compared to SDSS gi light curves in Fig. 4. Because the 2MASS data set is so large and we see no sign of Blazhko-modulation in the light curves, data are median-ed in 0.04 wide phase bins, with resulting random errors well below 0.01 mag. The variation of the light curve shape with bandpass wavelength seen in SDSS data (see Fig. 1), continues into near-IR, but only to the H band – the light curves in the H and K bands are barely distinguishable despite the high precision of 2MASS data. We proceed with a more detailed analysis of the JHK variability which reveals interesting light curve features.
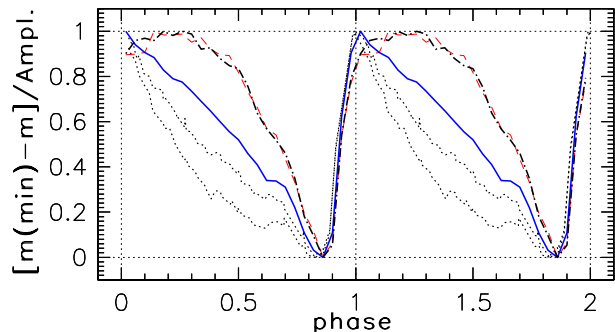

Figure 4. Phased and normalized SDSS gi and 2MASS JHK (bottom to top, respectively) light curves for SDSS$J015450 + 001501$. Phased 2MASS light curve data ($\sim$3000 data points per band) are median-ed in 0.04 wide phase bins, with resulting random errors well below 0.01 mag. SDSS light curves correspond to 64 data points each (with random errors of 0.01-0.02 mag), connected by straight lines. Note that the shapes of H and K light curves are barely distinguishable.

2.3.1. Phase-resolved near-IR color-magnitude hysteresis loops

The phased JHK light curves, the $J - K$ color variation with phase, and phased-resolved color-magnitude and color-color diagrams constructed with median-ed 2MASS data are shown in Fig. 5. A notable feature is that the time of maximum light in H and K bandpasses does not coincide with the time of maximum light

at shorter wavelengths, but lags in phase by about 0.25. Unlike the $J - K$ color which varies with an amplitude of $\sim$0.2 mag, the $H - K$ color does not appear to vary at all: its root-mean-square scatter is only 0.01 mag, and consistent with photometric noise (compare to 0.075 mag for the $J - K$ color).

Perhaps the most interesting feature revealed by the high-precision 2MASS data is seen in the J vs. $J - K$ color-magnitude diagram (bottom left panel of Fig. 5). In addition to the clearly seen "hysteresis" (for illustration of a similar behavior in the ugr bandpasses, see Figure 9 in Sesar et al. 2010), the $J - K$ color becomes bluer between phases 0.65 and 0.70 despite the decreasing brightness (see the middle right and bottom left panels, and arrow in the latter panel). Given the short duration ($\sim$45 minutes) and a small amplitude (0.03 mag) of this feature, it is unlikely that it was well observed for other stars. We return to an interpretation of this behavior in §2.5.
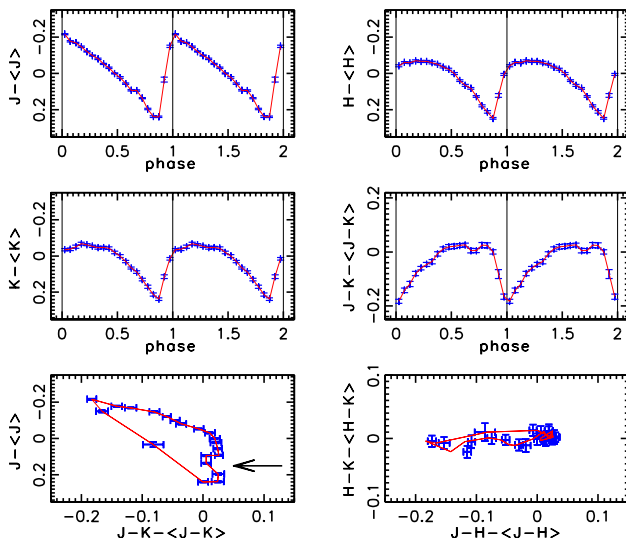

Figure 5. Top four panels display phased and normalized 2MASS JHK and color $J - K$ light curves for SDSS$J015450 + 001501$. Phased 2MASS light curve data ($\sim$3000 data points per band) are median-ed in 0.05 wide phase bins, with resulting random errors well below 0.01 mag. The median value of these averaged data points is subtracted from each curve, and points are connected by straight lines. Random errors are derived from scatter in each phase bin. Bottom two panels show color-magnitude (left) and color-color (right) hysteresis curves (the motion is clockwise). Note that between phases 0.65 and 0.70 the $J - K$ color becomes bluer despite the decreasing brightness (see the middle right and bottom left panels, and arrow in the latter panel). The $H - K$ color does not show any variation (rms of $\sim$ 0.01 mag, consistent with measurement errors).

2.4. *WISE light curve data*

The Wide-field Infrared Survey Explorer (WISE, Wright et al. 2010) mapped the sky at 3.4, 4.6, 12, and 22 μm. WISE imaged each point on the sky multiple times to achieve its sensitivity goals and to reject transient events such as cosmic rays. SDSS$J015450 + 001501$ was measured 43 independent times, during two epochs separated by approximately six months. The single-exposure photometric signal-to-noise ratio is high enough for light curve analysis in the W1 (3.4 μm) and W2 (4.6 μm)
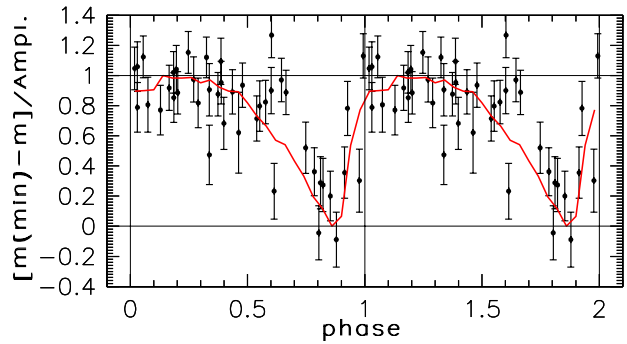

Figure 6. WISE $W1$-band phased and normalized light curve for SDSS$J015450 + 001501$ is shown as symbols with error bars (as computed by the WISE photometric processing pipeline). The line shows phased and normalized 2MASS K-band light curve (same curve as in Figure 4).

Table 4
WISE light curves for RR Lyrae star
SDSS$J015450 + 001501$ (43 epochs)

MJD	W1	$W1_{err}$	W2	$W2_{err}$
55209.272845	13.853	0.047	14.016	0.126
55209.405150	13.828	0.052	13.770	0.119
...	...	...	...	...

Note. — Table 4 is published in its entirety in the electronic edition of the Journal. A portion is shown here for guidance regarding its form and content.

bands: the median photometric errors are 0.05 mag for W1 and 0.15 mag for W2. These two light curves (43 data points per band) are compiled in Table 4.

Although WISE data are noisy, it is possible to make a rough comparison with 2MASS data. As shown in Fig. 6, the phased and normalized light curve in the W1 band is fully consistent with the corresponding 2MASS light curve in the K band (including the amplitude). A more detailed comparison of data across all ten bandpasses is described next.

2.5. *Simultaneous analysis of optical and infrared data*

As shown above, the shape of light curves varies greatly with wavelength. Another way to look at the same data set is to construct phase-resolved spectral energy distributions (SED). SEDs at minimum and maximum phases, and at phase=0.5, are compiled in Table 5 and shown in the top panel in Fig. 7. When the SED at phase=0.5 is scaled to a fainter flux level by 0.25 mag, it is indistinguishable from the SED at minimum phase (0.86). Assuming identical effective temperatures, this scaling factor implies that the effective radius of the star decreases by 12% between these two phases.

The variation of light curve amplitude with wavelength is shown in the bottom panel in Fig. 7. Between the SDSS g band (0.476 μm) and the 2MASS H band (1.65 μm), the amplitude steadily decreases from $\sim$1.3 mag to $\sim$0.3 mag. At longer wavelengths there is very little change of light curve amplitude, if any. The u band and the g band amplitudes are similar, which implies that the $u - g$ color stays approximately constant over the pulsational cycle. This is easily understood as the consequence of the fact that the $u - g$ color primarily

depends on metallicity (see Marconi et al. 2006).

The overall SED shapes are well described by static model atmospheres computed by Kurucz (1979). The solid lines in the top panel in Fig. 7 show Kurucz models for fixed $[Fe/H] = -1.5$ and log(g)=3.0, and best-fit $T_{eff} = 7500$ K (maximum light) and $T_{eff} = 6000$ K (minimum light). The effective temperature step in the model library was 250 K. A slight discrepancy between the measured u band magnitude at maximum light and the best-fit model can be reconciled as due to the impact of the steep SED in that region.

Figure 8. The symbols connected by dashed lines show 2MASS $J - K$ color vs. SDSS $g - i$ color for SDSS$J015450 + 001501$. Data were binned in 0.1 wide equidistant phase bins, and the bin centers are marked for a few data points (the motion during pulsational cycle is counter-clockwise in this diagram). Although both colors are good estimators of the effective temperature, a hysteresis is easily seen (e.g., at $g - i = 0$, about 0.05 mag difference in $J - K$ color). Note that both colors are essentially constant for phase bins from 0.45 to 085. The six thin solid lines are predictions based on Kurucz static model atmospheres with effective temperatures in the range 6000–7500 K. At the blue end, they bifurcate into the groups of three tracks – they correspond to models with $[Fe/H] = -1.5$ (the top three curves) and $[Fe/H] = -1.0$. For each metallicity, the three curves correspond to log(g)=2.5, 3.0 and 3.5. Note that at the blue end, the models bifurcate according to log(g), rather than $[Fe/H]$ (at $J - K \sim 0.13$, the $g - i$ color becomes bluer by ~ 0.1 mag as log(g) increases from 2.5 to 3.5).

Figure 7. Top panel: ten-band spectral energy distributions (SED) at maximum (top) and minimum (bottom) light for SDSS$J015450+001501$. Data are shown by symbols and connected by dotted straight lines. Open squares correspond to maximum light and open circles to minimum light (phase=0.86). Solid triangles, inside open circles, correspond to phase=0.50, *shifted fainter* by 0.25 mag. The SED *shape* at phase=0.50 is nearly indistinguishable from the SED at minimum light. The solid lines show Kurucz models for $[Fe/H] = -1.5$, log(g)=3.0, and $T_{eff} = 7500$ K (top) and $T_{eff} = 6000$ K (bottom). Bottom panel: light curve amplitude, in magnitudes, as a function of wavelength.

Despite this apparent success of static atmosphere models, it is easy to demonstrate that they cannot provide a complete description of the data. Fig. 8 shows a phase-resolved $J - K$ vs. $g - i$ color-color diagram. Both of these colors are by and large driven by effective temperature and Kurucz models show that the impact of log(g) is only minor (at most a few hundredths of a magnitude in the $J - K$ color at a given $g - i$ color, for a detailed discussion see Ivezić et al. 2008). Therefore, if static atmosphere models are sufficient to describe the data, then the data should follow a single line in this diagram, with the position along that line controlled by the effective temperature. In contrast, data in this color-color diagram show a similar hysteresis effect as the J vs. $J - K$ color-magnitude diagram (bottom left panel in Fig. 5). This color-color hysteresis, however, cannot be described as due to different stellar radii at a given effective temperature, as in the case of color-magnitude diagram.

To provide a precise quantitative estimate of the discrepancy between observed colors and colors predicted by Kurucz models, we compare a set of models for three
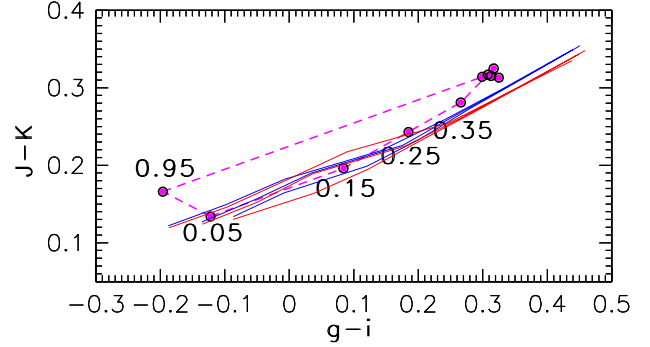
values of log(g) and two values of $[Fe/H]$ that bracket the values expected for this star (see Fig. 8). Models provide a fairly good agreement, to within a few hundredths of a magnitude) for the descending branch of the light curve (phases between the light curve maximum and minimum, the lower branch in Fig. 8). However, all models fail to explain the observed colors during the ascending branch, as the light curve goes from the minimum light to the maximum light (note that ascending portion of the light curve is about five times shorter than the descending portion). At a given $J - K$ colors, the discrepancy can be as large as ~ 0.2 mag!

Note that this model failing cannot be simply attributed to inadequacy of Kurucz models: whatever static atmosphere model library is invoked, it should produce much smaller hysteresis in this diagram, if any. For example, at a fixed $J - K = 0.2$, the difference in the $g - i$ color at the descending and ascending branches is over 0.2 mag. Similarly, at a fixed $g - i = 0$ color, the $J - K$ color differs by ~ 0.05 mag. Such large color differences are unlikely to be explained by the impact of log(g) parameter on static atmosphere models. It remains to be seen whether dynamic models can explain these data.

3. DISCUSSION AND CONCLUSIONS

Essentially by coincidence, the non-modulated (non-Blazhko) RR Lyrae star SDSS$J015450 + 001501$ has been extensively observed by several major sky surveys: SDSS, 2MASS, CSS, LINEAR and WISE. We have compiled data from these surveys and made the compilation publicly available in a user-friendly form. The light curves for this star are available in ten photometric bandpasses that span more than a factor of ten in wavelength and bracket the wavelength range where most of its luminosity is emitted. Light curves obtained by 2MASS stand out: they include close to 9000 photometric measures and provide an unprecedented precise view of near-IR vari-

Szabó et al.

Table 5
Spectral energy distribution data for RR Lyrae star SDSS$J015450 + 001501$

band	$\lambda_{\rm eff}$ (μm)	mag$_{\rm min}$	err	mag$_{\rm max}$	err	amplitude	mag$_{\phi=0.5}$	extinction corr.
u	0.3540	16.96	0.02	15.72	0.02	1.24	16.70	0.179
g	0.4760	15.78	0.01	14.51	0.01	1.27	15.52	0.139
r	0.6280	15.50	0.01	14.58	0.01	0.92	15.24	0.099
i	0.7690	15.38	0.01	14.66	0.01	0.72	15.14	0.075
z	0.9250	15.35	0.02	14.69	0.02	0.66	15.10	0.056
J	1.25	15.42	0.01	14.95	0.01	0.47	15.18	0.031
H	1.65	15.62	0.01	15.28	0.01	0.34	15.36	0.020
K	2.17	16.04	0.01	15.72	0.01	0.32	15.79	0.013
W1	3.4	16.80	0.05	16.46	0.05	0.34	16.56	0.008
W2	4.5	17.50	0.10	17.20	0.10	0.30	17.24	0.007

Note. — The table lists 2MASS and WISE magnitudes on AB scale. The following Vega-to-AB magnitude offsets ($m_{\rm AB}=m_{\rm Vega}+$offset) were used: 0.89, 1.37, 1.84 in JHK, and 2.6, 3.3 in $W1$ and $W2$. Magnitude values are not corrected for ISM dust extinction. Plausible extinction corrections (Schlegel et al. 1998) are listed in the last column and are derived using the SFD value for the r-band extinction quoted by SDSS for this star: $A_r = 0.099$, and coefficients listed in the first row of Table 1 from Berry et al. (2012) for the $ugrizJHK$ bands. For the WISE bands, the coefficients taken from Yuan et al. (2013) ($A_{W1}/A_r = 0.084$, $A_{W2}/A_r = 0.074$).

ability. A data set of similar completeness, precision, and wavelength and temporal coverage likely does not exist for any other RR Lyrae star.

The data for SDSS$J015450 + 001501$ presented here provide strong observational constraints for non-linear pulsation models of RR Lyrae stars. Sesar et al. (2010) already pointed out (see their Figure 8) that there are discrepancies between the $ugriz$ RR Lyrae light curves obtained by SDSS and theoretical light curve predictions from Marconi et al. (2006). Here, we further demonstrated that static atmosphere models are insufficient to explain multi-band photometric light curve behavior. Indeed, Barcza (2010) demonstrated that the quasi-static approximation is not valid for all phases during an RR Lyrae pulsational cycle. Pulsation models computed by Fokin & Gillet (1997) with a large number of mass shells in the stellar atmosphere show that the s3' and/or the merging s3+s4 shock waves might be at work at the pulsational phase range of 0.65-0.70, where we found the 'kink' in the $J - K$ color progression (Fig 5). We caution however that a large model survey should be conducted in a broad range of RR Lyrae physical parameters in order to verify the existence and the influence of these shock waves, in particular in SDSS$J015450 + 001501$.

Another complication is that in different passbands we observe the integrated light of different atmospheric layers. Therefore a frequency-dependent, dynamical atmosphere model coupled to a state-of-the-art hydrocode is needed to consistently handle the violent, shock-permeated outer parts of such large-amplitude pulsators. Frequency-dependent treatment of radiation hydrodynamics developed by Dorfi & Feuchtinger (1999) is very promising in this respect. They found good agreement between the synthetic optical RR Lyrae light curves and observations. An extension of such calculations to the near infrared passbands would be most beneficial for comparison with the data presented here.

REFERENCES

Abazajian, K. N., et al. 2009, Astroph. J. Suppl., 182, 543

Barcza, S. 2010, MNRAS, 406, 486

Becker, A. C., et al. 2008, MNRAS, 386, 416

Berry, M., et al. 2012, Astroph. J., 757, 166

Bono, G., Castellani, V., & Marconi, M. 2000, ApJ, 532, L129

Bramich, D. M., et al. 2008, MNRAS, 386, 887

Castelli, F., Gratton, R. G., & Kurucz, R. L. 1997, A&A, 318, 841

Cutri, R. M., et al. 2003, http://www.ipac.caltech.edu/2mass/releases/allsky/doc/

Davenport, J. R. A., Becker, A. C., Kowalski, A. F., Hawley, S. L., Schmidt, S. J., Hilton, E. J., Sesar, B., & Cutri, R. 2012, Astroph. J., 748, 58

Dorfi, E. A., & Feuchtinger, M. U. 1999, A&A, 348, 815

Drake, A. J., et al. 2013, Astroph. J., 763, 32

Fokin, A. B., & Gillet, D. 1997, A&A, 325, 1013

Ivezić, Ž., et al. 2008, Astroph. J., 684, 287

Ivezić, Ž., et al. 2007, Astron. J., 134, 973

Jester, S., et al. 2005, Astron. J., 130, 873

Kurucz, R. L. 1979, Astroph. J. Suppl., 40, 1

Lee, Y. S., et al. 2011, Astron. J., 141, 90

Marconi, M. 2009, in American Institute of Physics Conference Series, Vol. 1170, American Institute of Physics Conference Series (also arXiv:0909.0900), ed. J. A. Guzik & P. A. Bradley, 223

Marconi, M., Cignoni, M., Di Criscienzo, M., Ripepi, V., Castelli, F., Musella, I., & Ruoppo, A. 2006, MNRAS, 371, 1503

Nemec, J. M., Cohen, J. G., Ripepi, V., Derekas, A., Moskalik, P., Sesar, B., Chadid, M., & Bruntt, H. 2013, Astroph. J., 773, 181

Nemec, J. M., et al. 2011, MNRAS, 417, 1022

Plavchan, P., Jura, M., Kirkpatrick, J. D., Cutri, R. M., & Gallagher, S. C. 2008, Astroph. J. Suppl., 175, 191

Schlegel, D. J., Finkbeiner, D. P., & Davis, M. 1998, Astroph. J., 500, 525

Sesar, B., et al. 2010, Astroph. J., 708, 717

Sesar, B., et al. 2007, Astron. J., 134, 2236

Sesar, B., et al. 2013, Astron. J., 146, 21

Sesar, B., Stuart, J. S., Ivezić, Ž., Morgan, D. P., Becker, A. C., & Woźniak, P. 2011, Astron. J., 142, 190

Skrutskie, M. F., et al. 2006, Astron. J., 131, 1163

Wright, E. L., et al. 2010, Astron. J., 140, 1868

Yuan, H. B., Liu, X. W., & Xiang, M. S. 2013, MNRAS, 430, 2188

Szabó et al.

Table 6
SDSS *ugriz* light curves for RR Lyrae star SDSS J015450 + 001501 (64 epochs)

R.A.[a] (deg)	Dec[a] (deg)	MJD_u (day)	u (mag)	u_{err} (mag)	MJD_g (day)	g (mag)	g_{err} (mag)	MJD_r (day)	r (mag)	r_{err} (mag)
28.709058	0.250204	51075.379381	16.603	0.008	51075.381047	15.412	0.005	51075.377714	15.161	0.006
28.709058	0.250204	51818.349055	16.921	0.009	51818.350721	15.715	0.006	51818.347388	15.447	0.006
...	...	...	...	...	...	...	...	...	...	...

Note. — Magnitudes are not corrected for ISM dust extinction and set to -99.999 if unreliable. See Sesar et al. (2010) for more details. Table 6 is published in its entirety (including the *iz* photometry) in the electronic edition of the Journal. A portion is shown here for guidance regarding its form and content.
[a] Equatorial J2000.0 right ascension and declination.

Table 7
2MASS *JHK* light curves for RR Lyrae star SDSS J015450 + 001501 (2969 epochs)

SourceID	R.A.[a] (deg)	Dec[a] (deg)	BJD	J (mag)	J_{err} (mag)	J_{q}[b]	H (mag)	H_{err} (mag)	H_{q}[b]	K (mag)	K_{err} (mag)	K_{q}[b]
10038165	28.709000	0.250413	51003.4463211	14.257	0.030	A	14.007	0.041	A	13.947	0.075	A
10038255	28.708985	0.250394	51003.4466211	14.219	0.031	A	13.949	0.040	A	13.941	0.077	A
...	...	...	...	...	...	...	...	...	...	...	...	...

Note. — Table 7 is published in its entirety in the electronic edition of the Journal. A portion is shown here for guidance regarding its form and content.
[a] Equatorial J2000.0 right ascension and declination.
[b] Reliability flag. Single character flag that is related to the probability (P) that the extraction is a valid detection of a near infrared source on the sky at the time of the observation. "A" means P> 90%.